Cancer Management and Research

Dovepress
open access to scientific and medical research

Open Access Full Text Article

ORIGINAL RESEARCH

Securidaca–saponins are natural inhibitors of AKT, MCL-1, and BCL2L1 in cervical cancer cells

This article was published in the following Dove Press journal:
Cancer Management and Research

Titus Chukwuemeka Obasi,[1] Cornelia Braicu,[2] Bogdan Cezar Iacob,[1] Ede Bodoki,[1] Ancuta Jurj,[2] Lajos Raduly,[2] Ilioara Oniga,[3] Ioana Berindan-Neagoe,[2,4,5] Radu Oprean[1]

[1]Department of Analytical Chemistry and Instrumental Analysis, Faculty of Pharmacy, Iuliu Hatieganu University of Medicine and Pharmacy, Cluj-Napoca, Romania; [2]Research Center for Functional Genomics, Biomedicine and Translational Medicine, Iuliu Hatieganu University of Medicine and Pharmacy, Cluj-Napoca, Romania; [3]Department of Pharmacognosy, Faculty of Pharmacy, Iuliu Hatieganu University of Medicine and Pharmacy, Cluj-Napoca, Romania; [4]MEDFUTURE – Research Center for Advanced Medicine, University of Medicine and Pharmacy Iuliu-Hatieganu, Cluj-Napoca, Romania; [5]Department of Functional Genomics and Experimental Pathology, The Oncology Institute "Prof. Dr. Ion Chiricuta", Cluj-Napoca, Romania

Correspondence: Ioana Berindan-Neagoe
Research Center for Functional Genomics, Biomedicine and Translational Medicine, Iuliu Hatieganu University of Medicine and Pharmacy, 23 Marinescu Street, 400337 Cluj-Napoca, Romania
Tel +40 264 450 749
Fax +40 264 598 885
Email ioana.neagoe@umfcluj.ro

Radu Oprean
Department of Analytical Chemistry and Instrumental Analysis, Faculty of Pharmacy, Iuliu Hatieganu University of Medicine and Pharmacy, 4 Pasteur Street, 400349 Cluj-Napoca, Romania
Email roprean@umfcluj.ro

Introduction: Scientific research is beginning to prove the connection between claims by African traditional medicine and the natural chemical specifics contained in medicinal plant *Securidaca longipedunculata*. Our previous studies showed that two natural saponin fractions (4A3 and 4A4) identified in the plant as triterpenoid glycosides are capable of activating apoptosis on cervical tumor cell lines. Considering this and some critical roles of human papillomavirus (HPV) E6 oncogene on cervical cells, by promoting carcinogenesis and cell survival, it became necessary to investigate the possible pathways for apoptosis transmission.

Methods: Tests conducted on relevant cervical tumor cell lines such as Caski and Bu25TK included the following: MTT assay; scratch assay (to determine cell migration/invasion); fluorescence microscopy with Annexin V–fluorescein isothiocyanate, muscle progenitor cell) and propidium iodide staining; and finally reverse transcriptase quantitative PCR (RT-qPCR) for gene analysis.

Results: Reduced cell proliferation was observed due to activities of 4A3 and 4A4 fractions, with half-maximal inhibitory concentration (IC_{50}) of 7.03 and 16.39 µg/mL, respectively, on Caski cell line. A significant reduction in cell migration occurred within 48 and 72 hours, respectively, for Caski and Bu25TK cell lines. Late apoptosis was activated by 4A3, staining both Annexin V and PI, in contrast to 4A4's early apoptosis. RT-qPCR data revealed a fold change (FC) inhibition of antiapoptotic proteins such as MCL-1 and BCL2L1, with diminished level of AKT-3, VEGFA, MALAT1, etc. The expression of p53, proapoptotic BAD, and caspase-8 was nonsignificant.

Conclusion: The low expression of AKT-3 and antiapoptotic proteins (MCL-1 and BCL2L1), as well as VEGFA, could simply be an indication for possible suppression of cell survival mechanisms via multiple channels. We therefore conclude that 4A3 and 4A4 fractions mediate activity via the inhibition of phosphatidylinositol-3-OH kinase (PI3K)-AKT/mTOR/NF-κB-dependent antiapoptotic stimuli. Further studies are ongoing to reveal the chemical structures and compositions of these two fractions.

Keywords: early apoptosis, RT-qPCR gene analysis, AKT-3, MCL-1 and BCL2L1 inhibition, triterpenoid saponins

Introduction

Apoptosis is inherent in every cell, consisting of multistep complex pathways for programmed death of cells, serving as the mechanism for the removal of superfluous, aged, and damaged cells.[1–3] As a normal physiological process, it is required for the maintenance of cell homeostasis. The morphological hallmarks include loss of cell volume, hyperactivity of the plasma membrane, and condensation of peripheral heterochromatin, followed by the cleavage of the nucleus and cytoplasm into multiple membrane-enclosed bodies containing chromatin fragments.[4] In mammalian cells, the

submit your manuscript | www.dovepress.com
Dovepress
http://dx.doi.org/10.2147/CMAR.S163328

critical regulators of apoptosis are the Bcl-2 family members, which include antiapoptotic proteins such as Bcl-2 and Bcl-xL. They also include proapoptotic members, eg, Bad, Bid, and Bik of the BH3 subfamily, as well as the Bax and Bak.[5] Many antiapoptotic family members, including the Bcl-2 and Bcl-xL, are predominantly localized within the outer mitochondria membrane, while others interact directly or indirectly to maintain membrane integrity. Under normal circumstances, apoptotic cascade is initiated through the loss of permeability of the outer mitochondrial membrane accompanied by the release of cytochrome *c*. The release of cytochrome *c* from damaged mitochondria is coupled with the activation of caspase-9 and consequent release of caspase-3, a primary effector of apoptosis. Studies have shown that phosphatidylinositol-3-OH kinase (PI3K)-AKT pathway plays an important role in the regulation of Bax cytosol localization, preventing its translocation into mitochondria via PI3K activity.[6,7] Through this means, the PI3K-AKT pathway plays a strong role in promoting cell survival. Emerging as a major pathway to cell survival, the activation and phosphorylation of AKT have been linked to diverse antiapoptotic stimuli, leading to the blocking of apoptosis in several cells.[8] The inhibition of apoptosis by AKT sometimes can be in caspase-independent manner through the delay of the release of cytochrome *c* from mitochondria or delay of the activities of several proapoptotic Bcl-2 family members.[9] Therefore, the expression of Bcl-2 family members (Bcl-xL and Bcl-2) is very important for cell survival and protection of the integrity of mitochondria.

The PI3K-AKT signaling pathway is a critical regulator of many cellular processes that promote cell survival, tumorigenesis, and malignant transformation of normal cells. With the mechanism of cell survival, there is an active inhibition of apoptosis, in which the expression of proapoptotic factors is constantly depressed on the one hand, while on the other hand promoting antiapoptotic transmission. Inhibition of apoptosis is championed through the activation of EGFR-PI3K-AKT signal transduction. Perhaps, due to the loss or compromised function of PTEN (phosphatase and tensin homolog), a tumor suppressor acting at the PI3K-AKT transmission checkpoint. One of the possible reasons for the loss of PTEN activity in cervical cancer could be related to the actions of miR-21. As a true oncomir, miR-21 is a gene regulator at the post-transcriptional level, being overexpressed in different types of malignancies, including human papillomavirus (HPV)-positive cancers.[10,11] Research findings have shown that miR-21 is a known oncogene that negatively regulates PTEN to effect cell survival and tumorigenesis through the activation of PI3K-AKT. As several miRs are indicated for PTEN deficiency, research findings have also shown that elevated or decreased expression of miR-21 mediates direct effect on cell proliferation, differentiation, and apoptosis.[12–14] This claim, however, has been verified by the reduced expression of miR-21 in the normal cytology of HPV-negative tissues, compared with the positive or abnormal tissues.[10] Hence, they express higher in conditions such as squamous cell carcinoma (SCC) than the common HPV-negative cervicitis. Considered as a major driving factor for the carcinogenesis of cervical cells, the E6 oncogene in addition has its molecule implicated in the deactivation and degradation of important tumor suppressor genes and proteins, eg, the p53 (guardian of the genome), pRb, and programmed cell death (PDCD4), whose functions promote apoptosis and cell cycle arrest.[15,16] This, however, has been further verified by the molecular inactivation and degradation of p53 tumor suppressors by E6, through binding interaction between the E6, the associate protein (E6-AP), and p53 at the consensus binding site, to form a ternary complex frequently prone to ubiquitination.[15] Based on these facts, blocking the cell survival strategies and the diverse roles of E6 molecules could be seen as viable therapeutic target for the restoration of p53 functioning. Similarly, it is expected that any target to E6 will also affect the EGFR overexpression, which is normally activated through hippo/Yap pathway.[17] Signals from the activated PI3K-AKT pathway usually result in phosphorylation of AKT, the role of which is diverse in regulating tumor proliferation via the downstream respondents, such as mTOR- and NF-kB-dependent antiapoptotic protein expression.

Materials and methods

Plant materials

The dried root part of *Securidaca longipedunculata* weighing about 1.2 kg was supplied by Mr John Apev of the Department of Medicinal Plants Research and Traditional Medicine, National Institute for Pharmaceutical Research and Development (NIPRD), Idu, Abuja, Nigeria. The voucher specimen number as retained in the herbarium (Ethnobotany unit) of the NIPRD is specified as follows: NIPRD/H/6576.

Extraction and fractionation

Bioactivity-guided extraction was applied on the pulverized root part of *S. longipedunculata* to obtain an extract which was purified by fractionation using a method described in the study by Obasi et al.[18] In this case, 100.050 g of pulverized root powder of *S. longipedunculata* was thoroughly defatted with 500 mL of dichloromethane (DCM) for 24 hours,

using Soxhlet apparatus to remove the undesirable lipids. Residual solvent in the plant material was totally removed by air-drying before re-extracting with pure methanol for 48 hours. A residue of 12.612 g was recovered under reduced temperature in a rotary evaporator. About 5.045 g of the residue was completely dissolved in 200 mL of distilled water in a flask and dispersed for 30 minutes in ultrasonic bath. The resultant aqueous mixture was then mixed with 400 mL ethyl ether with vigorous agitation to form emulsion. The content was transferred into a separating funnel for phase separation to take place at room temperature. After 24 hours, phase separation was completed, forming a creamy precipitate at the middle interface, while leaving a clear bright yellow upper phase (ethyl ether) and reddish brown clear aqueous phase. This middle fraction labeled 4A was carefully collected and centrifuged at low speed of 14.5 rpm, and the supernatant liquid was discarded while the solid residue at the bottom was dried under low temperature using Eppendorf Concentrator Plus (Eppendorf, Hamburg, Germany). The cream-colored dried 4A was further purified by repeating the same process until the color became whiter and the level of impurities reduced to about 10% measuring with a ultraviolet (UV)–visible spectrophotometer, as described in the study by Obasi et al.[18] MTT assay was conducted on purified 4A using Caski cell line, and the presence of saponin was confirmed by relevant phytochemical tests which included foam test, post-thin layer chromatography (TLC) derivatization with 10% H_2SO_4 ethanolic solution, p-anisaldehyde, Carr-Price, Liebermann–Burchard reaction, and thymol–H_2SO_4, which was treated on the acid-hydrolyzed portion. The purified 4A was further fractionated to isolate 4A3 (0.045 g) and 4A4 (0.33 g) by reversed-phase preparative TLC.

TLC separation and characterization

The best parameters and developing system for TLC separation of 4A were first established using analytical system. Silica gel 60 RP-C18, $F_{254}S$ (EMD Millipore, Billerica, MA, USA), was selected as stationary phase, and methanol–water–formic acid (4:1:0.1, v/v) system as mobile phase. Chromatograms were examined under normal light and UV 365 nm, derivatized by spraying of 10% (w/v) ethanolic H_2SO_4, a modified method of Fenwick and Oakenfull (1981).[40] Saponin spots were visualized upon heating at varied range of temperatures for 3- and 6-minute intervals and above. When all the parameters were ascertained, preparative TLC (glass plate) silica gel 60 RP-C18, $F_{254}S$ (20 cm × 20 cm), 1 mm layer thickness, was introduced for the purpose of isolating the constituents. Limited exposure to light was maintained while carefully scraping the bands from the developed plate. Relevant bands were collected as powders, eluted with methanol, and recovered back into dryness under low temperature. These TLC fractions were subjected to MTT test, and the most relevant ones were engaged in post-TLC derivatization with 10% ethanolic H_2SO_4, antimony (III) chloride (Carr-Price), p-anisaldehyde sulfuric acid, and Liebermann–Burchard's reagents as well as thymol–H_2SO_4 on the acid-hydrolyzed portions. The volume distribution of the bands was also determined to estimate the percentage of occurrence.

Cell culture

CASKI cell line and Bu25TK cervical cancer cells were used for the experiments, and these were purchased from American Type Culture Collection (ATCC, Manassas, VA, USA) cell bank. These cells were cultured in Gibco RPMI 1640 Medium 1X, supplemented with 10% FBS (Thermo Fisher Scientific, Waltham, MA, USA) and 1% penicillin–streptomycin. Cell lines were maintained at 37°C and 5% CO_2 in a humidified incubator.

Cell proliferation evaluation by MTT test

The MTT assay was performed to evaluate the biological activity of the TLC fractions as basic screening test for identifying the bioactive substances. Then, the half-maximal inhibitory concentration (IC_{50}) was evaluated using multiple doses of the most bioactive fractions on the aforementioned cell lines. The MTT salt was cleaved by dehydrogenase in the living cells and was reduced to an insoluble formazan crystal which showed a specific purple color. The color was detected by a plate reader (Synergy H1 Hybrid Reader; Biotek, Bad Friedrichshall; Germany). Caski and Bu25TK cells were seeded overnight in 96-well plates at an 8×10^3 cells/well density, and then cells were treated with corresponding doses of the TLC fractions and incubated for another 24 hours. Cell suspension was removed; 150 µL MTT solution was added and incubated for 1 hour; the solution was removed; 100 µL dimethyl sulfoxide (DMSO) was added to dissolve the formazan product and incubated at 5–10 minutes in a plate shaker. After the incubation, the absorbance was measured at 570 nm in a plate reader (Synergy H1 Hybrid Reader). Using the following formula, the inhibition rate was calculated: Y (%) = (1–T/C)×100, where Y is the growth ratio of cancer cell mortality at each sample concentration, T is the mean absorbance of treated cells, and C is the mean absorbance of negative control. This formula showed the IC_{50} value, where the concentration of the fractions 4A3 and 4A4 caused 50%

growth inhibition. The IC_{50} value (the value at which 50% of cells are dead as response to treatment exposure) was calculated using GraphPad Prism as a standard value for toxicological tests.

Autophagy and apoptosis evaluation by fluorescence microscopy

Autophagy was evaluated by microscopy using dual staining with monodansylcadaverine (MDC) and propidium iodide (PI) staining. MDC is a specific marker for autophagy vacuoles, while PI staining emphasizes the necrotic cells. The apoptosis was evaluated with Annexin V–fluorescein isothiocyanate (FITC; Cayman Chemical, Ann Arbor, MI, USA) and PI kit (Cayman Chemical), and necrotic and apoptotic cells were detected by fluorescence microscopy for the selected treatment scenarios. The cells were seeded in 96-well plates in a number of 10^4 cells/well and were treated 24 hours later with a single dose of the most effective fraction (4A3 and 4A4); all evaluations were performed in triplicate.

In vitro cell migration assay

The cervical cancer cell lines were treated with the most effective phytochemical fractions (4A3 and 4A4) to monitor the process of healing of the "wound gap" created for assessing cell migration potential. Caski and Bu25TK cells were grown in DMEM supplemented with 10% FBS for 24 hours to form a confluent monolayer in 24-well plates before making straight scratch (with p100 tips) on the surface. After washing to remove the detached cells, each well was replenished afresh with specific medium containing 10 µg/mL 4A3 and 4A4 to inhibit cell proliferation. Cells were grown for additional 48 and 72 hours for Caski and Bu25TK, respectively. At 0, 6, 24, 30, 48, and 72 hours, the "gap width" of the scratch repopulation was measured and recorded and then compared with the initial gap size at 0 hour and that of the untreated cells (control).

RNA extraction, quality control, and assessment of gene expression using quantitative reverse transcriptase PCR (qRT-PCR)

For the extraction of total RNA, we used the TriReagent (Sigma-Aldrich Co., St Louis, MO, USA) protocol. The quantitative and qualitative control was performed using the Nanodrop-1000 spectrophotometer (Thermo Fisher Scientific) and the Agilent Bioanalyzer 2100 (Agilent Technologies, Santa Clara, CA, USA). cDNA synthesis was performed using the High-Capacity cDNA Reverse Transcription Kit (Thermo Fisher Scientific) and SuperScript III Reverse Transcription (Thermo Fisher Scientific), according to the manufacturer's recommendations. For the RT-qPCR, we used the SyBR Select Master Mix and the ViiA 7 instrument from Thermo Fisher Scientific. Specific primers were used for each gene of interest, VEGFA, AKT3, MCL-1, GAS5, TP53, MALAT1, BAD, CDH1, BCL-XL, and CASP8, as well as for the housekeeping genes, B2M and GAPDH (Table 1). Alterations of gene expression levels for the studied genes were evaluated using the ΔΔCt method.

BCL-2 and VEGF protein expression quantification

The expression level of BCL-2 protein was assessed by immunostaining overnight with monoclonal BCL-2 primary antibody (10 µg/mL, AF810; R&D Systems, Inc., Minneapolis, MN, USA), followed by a washing step with phosphate-buffered saline and incubation for 2 hours with anti-mouse FITC secondary antibody (10 µg/mL, MAB8980; R&D Systems, Inc.); washing and evaluation were performed by confocal microscopy. The quantification of VEGF released in cell culture medium was done using ELISA kit (DVE00; R&D Systems, Inc.) based on the recommended manufacturer's protocol.

Table 1 Primer sequences used for qRT-PCR analysis

Gene name	Primer sequence
VEGFA	TCTCCGCTCTGAGCAAGG
	TGCCCGCTGCTGTCTAAT
AKT3	CATAATTTCTTTTGCATCATCTGG
	TTGCTTTCAGGGCTCTTGAT
MCL-1	GCAGCACATTCCTGATGCCACCT
	ACGCGGTAATCGGACTCAACCT
GAS5	CAAGCCGACTCTCCATACCT
	CTTGCCTGGACCAGCTTAAT
TP53	CCCTTTTTGGACTTCAGGTG
	AGGCCTTGGAACTCAAGGAT
MALAT1	TTATGGATCATGCCCACAAG
	GACCCTTGACCCCTCACC
BAD	GCTTCCTCTCCCACCGTAG
	ACCCGGCAGACAGATGAG
CDH1	GATGGCGGCATTGTAGGT
	GGTCTGTCATGGAAGGTGCT
BCL2L1	GCGATCCGACTTCACCAATAC
	CCCAGAAAGGATACAGCTGG
CASP8	TTTCTGCTGAAGTCCATCTTTTT
	TAGGGGACTCGGAGACTGC
B2M	CCTCCATGATGCTGCTTACATG
	CACCCCCACTGAAAAAGATGAG
GAPDH	CACCTTCCCCATGGTGTCT
	CCCCGGTTTCTATAAATTGAGC

Abbreviation: qRT-PCR, quantitative reverse transcriptase PCR.

Results

Bioactive constituents' extraction and identification

Through a bioactivity-guided method, relevant cytotoxic fractions were retrieved from the root part of *S. longipedunculata* and screened for necessary biological activity. Figure S1 shows the bioactivity-guided extraction process. The basic chemical identification of the bioactive triterpenoid saponin by post-TLC derivatization is given in Table S1 and Figures S2–S5. In the nonchemically derivatized plate, the chromatogram showed the characteristic blue fluorescent spots under UV 365 nm. After treatment with 10% ethanolic H_2SO_4 and heating at 105°C for 3 and 6 minutes, the former nonvisible fractions became seen under UV 365 nm as blue–violet spots. The post-TLC derivatized fractions (1–5) confirmed the presence of triterpenoid saponin by p-anisealdhyde–H_2SO_4, Liebermann–Burchard, and Carr-Price tests, with characteristic color reactions for triterpenoid aglycone. The sugar portion (glycone) was revealed after acid hydrolysis and treatment with thymol–H_2SO_4. Analysis further showed the respective percentage distribution of 4A (3 and 4) as (6.35 and 50.04)% v/v of the total volume of 4A.

Cell proliferation inhibition assay

Within the 24 and 48 hours post treatment, MTT test revealed a reduced cell proliferation, particularly on Caski cell line. Among the fractions tested, 4A3, 4A4, and 4A5 maintained the strongest anti-proliferative effect, thus they were chosen for further evaluations. The cell viability and specific data relating to IC_{50} of fractions 4A3, 4A4, and 4A5 are presented in Table 2 and Figure 1.

Autophagy and apoptosis evaluation on Bu25TK and Caski cells

Fluorescence microscopy showed significant cell alterations 48 hours after treatment (Figure 2). The untreated cells did not show any staining, suggesting that no significant apoptosis or necrosis took place. Data further suggested much more cell death with 4A3 in particular, which may be related to

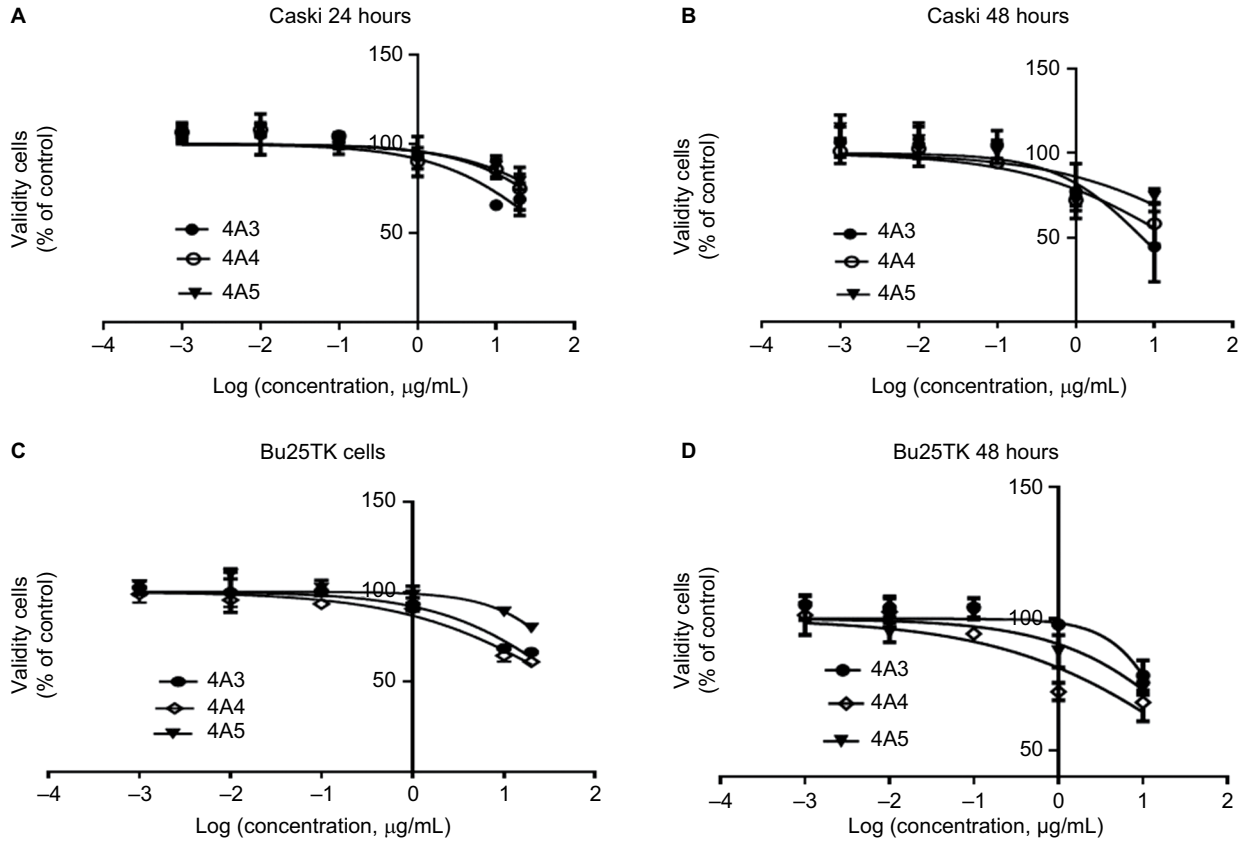

Figure 1 Cell viability measured by MTT assay.

Notes: (**A**, **B**) Caski cell line and (**C**, **D**) Bu25TK cell line after 24- and 48-hour treatment, respectively. Data are expressed as the percentage of control after 24 and 48 hours, in incubation with different concentrations of the most effective fraction (4A3, 4A4, and 4A5) on Bu25TK and Caski cell lines; log(concentration, μg/mL) = log(concentration of bioactive fraction, μg/mL) (mean ± SD, n=3).

Table 2 The IC_{50} values of 4A3, 4A4 and 4A5 fractions on Bu25TK and Caski cell lines

Cell line	Fractions	Time (hours)	IC_{50} (μg/mL)	Slope	R^2
Bu25TK	4A3	24	48.65	0.1229	0.9002
		48	28.65	0.7956	0.8051
	4A4	24	43.93	0.05565	0.9466
		48	48.59	0.09214	0.7773
	4A5	24	75.32	0.3096	0.7558
		48	62.72	0.1409	0.8048
Caski	4A3	24	50.40	0.1973	0.7883
		48	7.034	0.2535	0.7644
	4A4	24	112.9	0.3281	0.6871
		48	16.39	0.09467	0.8452
	4A5	24	188.1	0.2842	0.6896
		48	63.16	0.2245	0.5474

Note: IC_{50} values determined by MTT test after 24 and 48 hours of treatment with fractions 4A3, 4A4, and 4A5 on Bu25TK and Caski cell lines.
Abbreviation: IC_{50}, half-maximal inhibitory concentration.

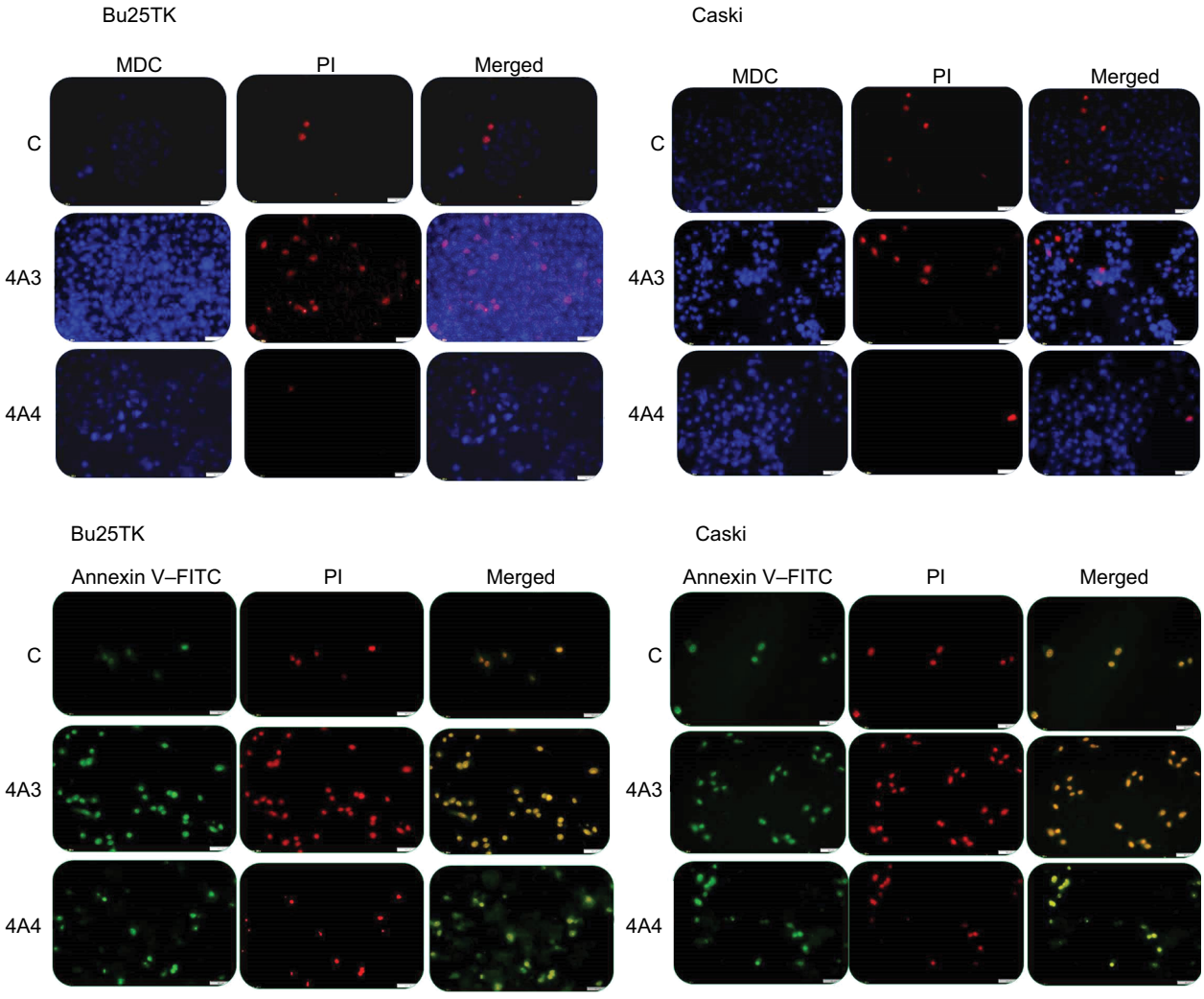

Figure 2 Autophagy and apoptosis assessment by fluorescence microscopy.
Notes: Cells were treated for 48 hours with a single dose of 4A3 and 4A4 on Bu25TK and Caski cell lines. 4A3 shows the late apoptosis staining, both Annexin V (green) and PI (red), while 4A4 shows the preferentially stained Annexin V–FITC (20× magnification).
Abbreviations: C, control; FITC, fluorescein isothiocyanate; MDC, monodansylcadaverine; PI, propidium iodide.

the activation of autophagy and apoptosis. Late apoptosis was displayed by 4A3 with dual staining for both Annexin V (green) and PI (red), while 4A4 preferentially stained only for Annexin V, indicating early apoptotic cells. These facts were observed on both cell lines.

Inhibition of cervical cancer cell migration

The in vitro cell migration studies by scratch wound-healing assay indicated a reduction in migration capacity on the two cervical cell lines (Figure 3). Our data revealed that cells treated with 4A3 and 4A4 fractions were related to approximately 50% reduction in migration in Caski cell line within 48 hours, while Bu25TK in 72 hours showed a relatively reduced migration amounting to 15.81% and 23.58% area of the scratched surface.

Relative gene expression quantification in response to treatments

The level of expression of eight genes (AKT3, BAD, CDH1, MCL-1, TP53, BCL2L1, CASP8, and VEGFA) and two long noncoding RNA transcripts (GAS5 and MALAT1) by TaqMan RT-qPCR assay is shown in Figure 4. The primer sequence of the genes is presented in Table 1, while their relative expression was calculated using the Ct method, by dividing the Ct target gene to Ct housekeeping gene (*B2M* and *GAPDH*) for the selected genes and long noncoding transcripts. Between the groups, there was no statistically significant alteration for apoptotic proteins, BAD, CASP8, and TP53 on both tested fractions and variant cells. For the antiapoptotic proteins, MCL-1 and BCL2L1, there was a significant inhibition of expression. In the case of 4A3, a fold change (FC) of 0.1481±0.1405 and 0.5563±0.1077, respectively, on Caski and Bu25TK cells was achieved. The 4A4 maintained 0.5359±0.1932 and 0.6725±0.07639 inhibition, respectively, on both cell lines. The AKT3 was significantly inhibited. AKT, which is a gene that controls cell proliferation, differentiation, and apoptosis in cervical cancer, was downregulated as a result of exposure to both fractions in Bu25TK cells, while in Caski cells expressed only as response to 4A3 treatment. Bu25TK is a classical derivative of Hela, positive with HPV. In the case of the genes related to angiogenesis and invasion, VEGFA was sig-

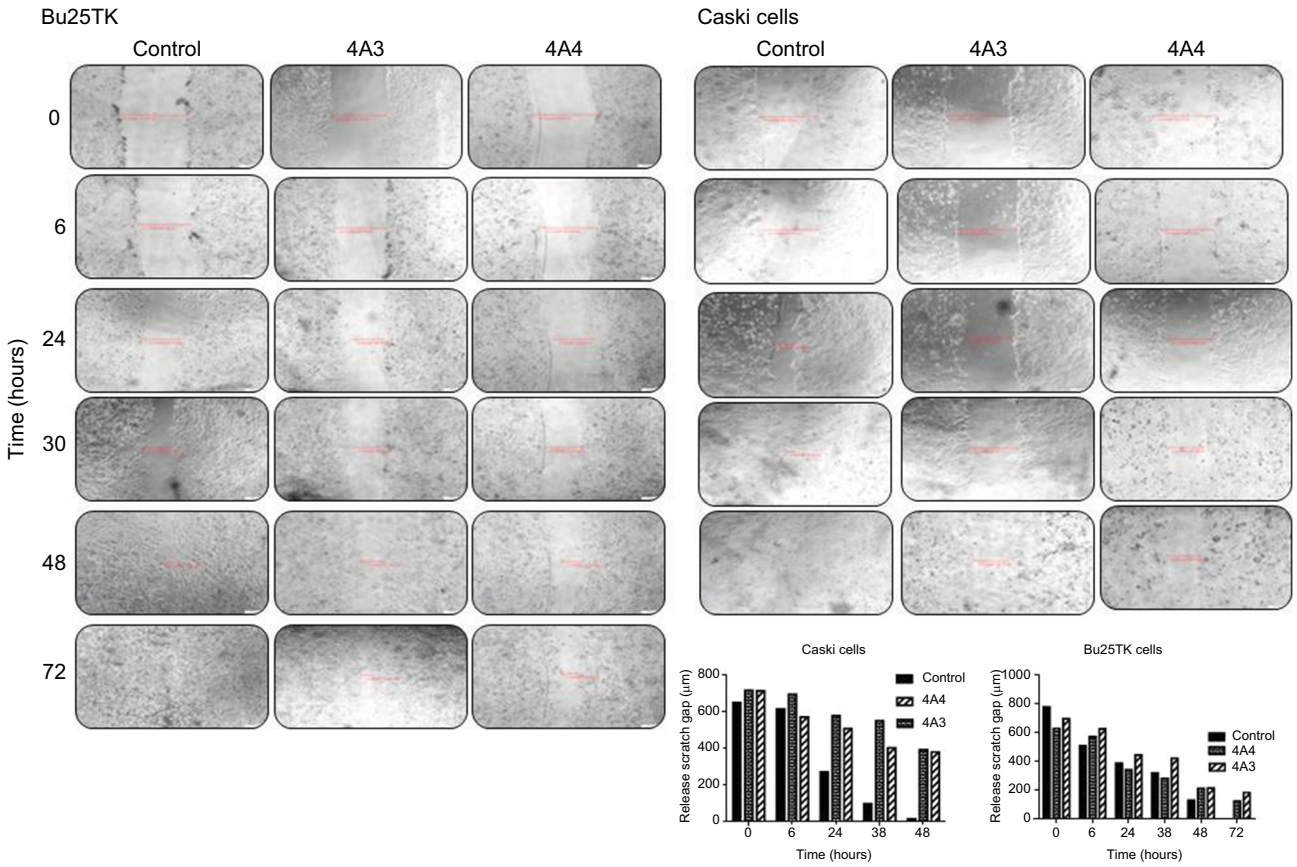

Figure 3 In vitro scratch assay.
Notes: Cell migration evaluated on Bu25TK and Caski cell lines treated with 4A3 and 4A4, respectively, and different time points (4× magnification).

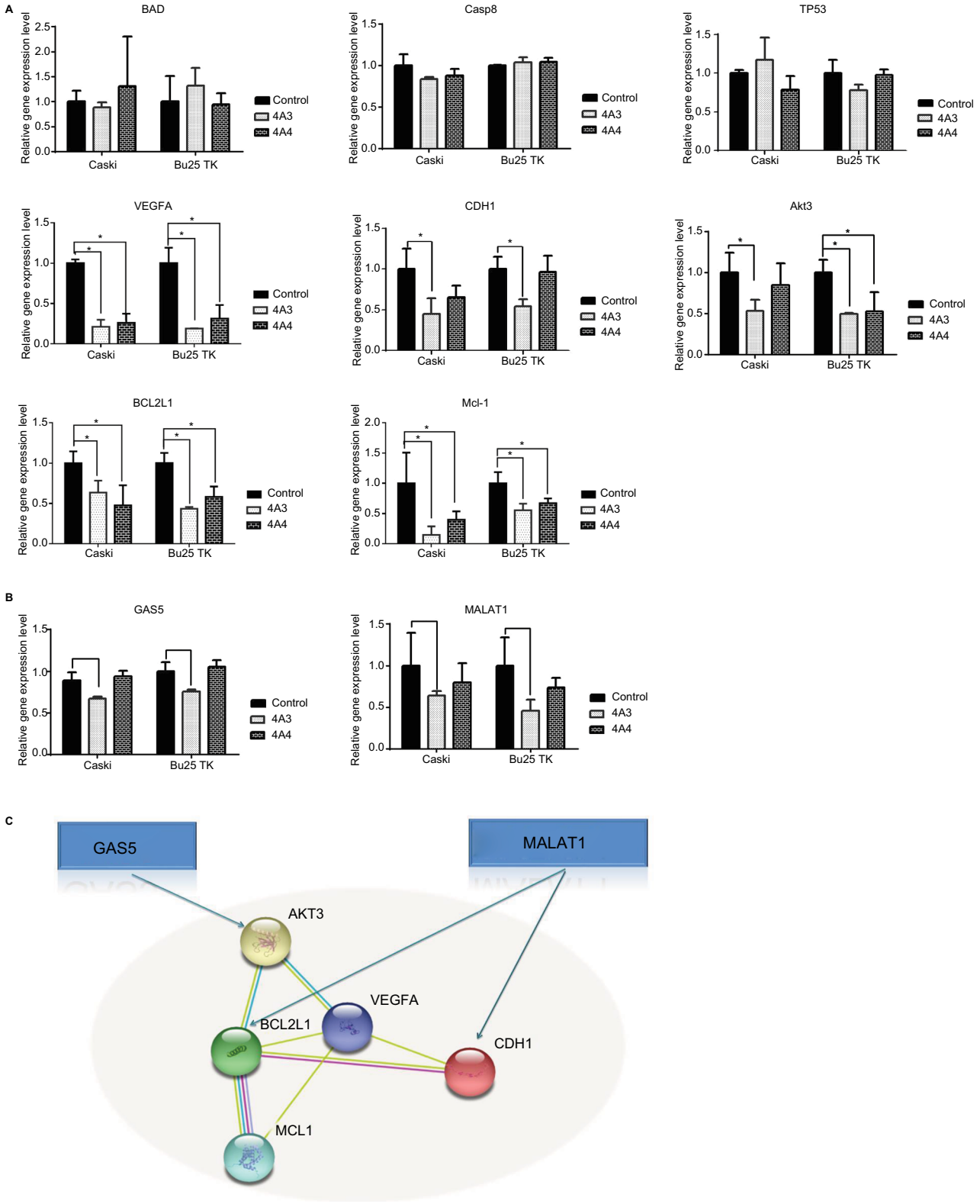

Figure 4 Gene expression.

Notes: (**A**) Evaluation of response due to treatment with 4A3 and 4A4 at 24 hours. (**B**) Gas5 and MALAT1 expression level for same treatment scenarios. (**C**) String network for the transcripts with altered expression level. Data are generated using default settings (medium confidence of 0.4). *$P \leq 0.05$.

nificantly downregulated by the treatment of both fractions, while CDH1 was downregulated only by 4A3. The string network (Figure 4C) predicts all direct and indirect connections of genes with altered expression. This further suggests that 4A3 and 4A4 extract targets multiple genes and proteins that often act in synergy for enhanced apoptosis and reduced capacity for cell proliferation and invasion.

BCL-2 and VEGF protein expression quantification

The expression level of BCL-2 protein was assessed by immunostaining using specific antibodies, primary antibody, followed by confocal microscopy evaluation. The secondary antibody that was specifically linked to the specific antibody for BCL-2 protein was emitting green fluorescence. It was demonstrated a cytosolic localization of BCL-2 protein; the intensity of signal was more intense in the control group (Figure 5A). In the case of 4A3- and 4A4-treated cells, we had a reduced expression level of VEGF in the cell culture medium (Figure 5B).

Discussion

According to WHO traditional medicine strategy (2002–2005), it is a stark reality that not less than 80% of the world's population, particularly in Africa, Asia, and low- and middle-income countries, still depend totally on natural medicine for their health care needs.[19] The traditional knowledge, which has served mankind for centuries in these regions, cannot be easily dismissed, as scientific research is beginning to prove the connection between their claims and the natural chemical specifics contained in plants. Some natural plant-derived compounds exhibit inhibitory action against HPV-induced carcinoma through the mediation of apoptosis. This has been verified in many compounds such as soyasaponin, methyl jasmonate, phytoglycoprotein, curcumin, and epigallocatechin gallate (EGCG).[2,20–24] Podolak et al,[25] in their review, further summarized the pharmacological properties, including the wide range of cytotoxic activities of different saponosides on tumor cell lines. For non-HPV tumor cells such as human ovarian cancer (A2780 cell line), oleanane-type triterpenoid saponins from Albizia gummifera have also been found to induce apoptosis, just as those of Albizia adianthifolia (Mimosaceae) the activity of which enhances apoptosis on human leukemia T cells (Jurkat cells) and splenocytes.[26,27]

In this study, we found that two saponin fractions labeled 4A3 and 4A4, isolated from *S. longipedunculata* (Polygalaceae), mediate apoptosis against tumorous cervical cell lines, Caski and Bu25TK. Before now, about eight or more different types of saponins of mainly C30 aglycones have already been isolated from this plant, supporting the great work of Mitaine-Offer et al,[28] Lenz,[29] and Johnson[30] who suggested that *S. longipedunculata* is very rich in both acidic and neutral saponins. This further justifies the claims for use of this plant in the treatment of cancer in African traditional medicine.[31] From our result, an IC_{50} of 7.034 and 16.39 µg/mL was achieved within an interval of 48 hours in Caski by 4A3 and 4A4, respectively, agreeing with similar report by Berindan-Neagoe et al,[3] as related to the induction of apoptosis with plant natural products at minimal doses. The 4A4 fraction was quite

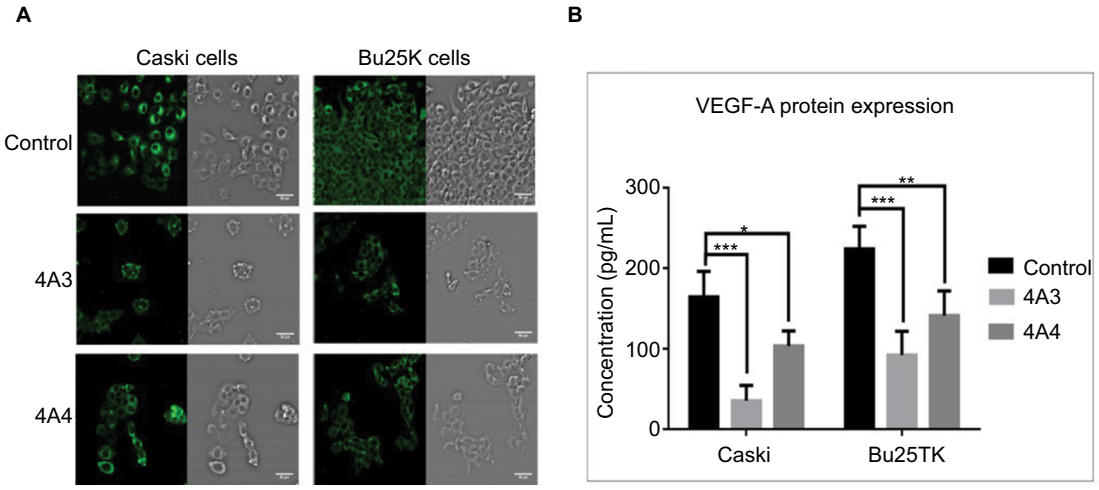

Figure 5 BCL-2 and VEGF protein expression quantification.
Notes: (**A**) Confocal microscopy for BCL-2 immunostaining for control and 4A3- and 4A4-treated CASKI and Bu25TK cells for 48 hours post treatment in eight-well chamber slides (20× magnification). (**B**) VEGF quantification from cell culture medium was performed using ELISA for same experimental groups at 48 hours post treatment. *$P \leq 0.05$; **$P \leq 0.01$; ***$P \leq 0.001$.

selective, causing early apoptosis on both cell variants, compared with 4A3 non-differential staining of Annexin V and PI, which indicates late apoptosis or necrotic cell death. Emphasizing the role of E6 molecule in promoting cell survival at the expense of apoptosis, it became necessary to monitor the level of expression of AKT, MCL-1, and BCL-2 antiapoptotic proteins as well as the VEGFA and other relevant genes (Figures 4 and 5). The major reason for carrying out this activity was based on the fact that E6 molecule stimulates cell survival signals, through the overexpression of EGFR and deregulation of the activity of PTEN tumor suppressor, the function of which is to regulate PI3K-AKT pathway.[17,32]

As a matter of fact, the inactivation of PTEN in cervical cancer is frequently driven by the overexpression of miR-21 causing the dismantling of the regulatory checkpoint at the PI3K-AKT pathway.[13,15] The phosphorylation of AKT has been linked to several activities leading to cell survival and tumorigenesis, with implication on apoptosis. However, our data shown in Figure 4 revealed that AKT is strongly inhibited by *Securidaca*–saponin fractions. As one of the possibilities promoting cervical cancer, the PTEN activation might have been obstructed via miR-21- and E6-dependent activities. In this study, we need sufficient data to make the necessary proof, as we plan to go for detailed studies in the future. AKT is a serine/threonine kinase, the role of which is reputable for central antiapoptotic transmissions, which encompasses the promotion of cell proliferation, differentiation, angiogenesis, and cell invasion. The signal transduction of AKT and its activation has been widely implicated in drug therapy resistance and found responsible for promoting malignant phenotype.[33] AKT regulated the activities of proapoptotic protein BAD the expression of which was found nonsignificant on both the cell lines (Figure 4). The inhibition of the downstream antiapoptotic proteins, such as MCL-1 and BCL-2, affected the permeability of the mitochondrial membrane, leading to the translocation of proapoptotic Bax and Bak and initiation of apoptosis. In a strong term, we maintained assumptions that signal transductions via AKT-mTOR pathway may have been the possible reason for the "switch on" of proapoptotic machinery in this case, given the diminished gene expression level of MCL-1, VEGFA, and MALAT1 and protein level in the case of BCL-2 (Figures 4 and 5). Although not exactly the same, it has been reported that MALAT1 enhances pro-angiogenic effect of VEGFA and FGF2, acting via the MALAT1/mTOR/HIF-1α pathway.[34]

These molecular targets, especially the PI3K-AKT, mTOR, and NF-κB, are very important factors in most types of cancers and have been studied extensively for the purpose of anticancer development. In justifying this, we found that despite the nonsignificant expression of p53 or BAD (Figure 4), apoptosis still took effect due to diminished level of antiapoptotic proteins, which stimulated mitochondria apoptosis, transactivation of Bax, and the release of cytochrome *c* and caspases. Even though the expression of p53 often times denotes poor prognosis in cervical cancer, the nonsignificant alteration (Figure 4) clears the doubt of any implication relating to genotoxicity as a result of treatment.[35–37] While caspase-8 expression is also nonsignificant (Figure 4), there is no concrete evidence to suggest that proapoptotic transmission involved the passages through the death receptors (ie, the extrinsic apoptotic pathway). Therefore, we propose that each of the saponin fractions could be harboring potential chemical agent(s) that target against E6 molecular activities, leading to the restoration of p53. On the other hand, it can also be suggested that the activation of PTEN tumor suppressor may be highly indicated, considering its functional regulatory role mounted at the PI3K-AKT checkpoint, which is very essential for the downregulation of antiapoptotic stimuli via mTOR/NF-KB (Figure 6A and B). More importantly, it is very clear that E6 oncoprotein which promotes the inhibition of PTEN via miR-21 activity is highly expressed only in diseased cells.[38,39] Further studies are ongoing to reveal the chemical structures and composition of these two bioactive saponin fractions. Finally, we consider that metabolized products of natural compounds can equally be contributing to substantial therapeutic potential.

Conclusion

We suggest that the depth of activity of 4A3 and 4A4 is culminated into AKT downregulation, with the principal-dependent antiapoptotic proteins (MCL-1 and BCL2L1), which by implication may have their activity exerted through mTOR- and NF-κB-dependent pathways, respectively. Therefore, we consider the ability of these fractions to kill tumor cells and induce apoptosis in a manner involving multiple regulatory pathways, a boost to their potentials against tumors, making them attractive as candidates for anticancer development and valuable source for developing new derivative compounds with increased therapeutic efficacy.

Acknowledgment

This work was supported by the Iuliu Hatieganu University of Medicine and Pharmacy (UMF), Cluj-Napoca, Romania, through a PhD Project Research grant (7690/81/15.04.2016).

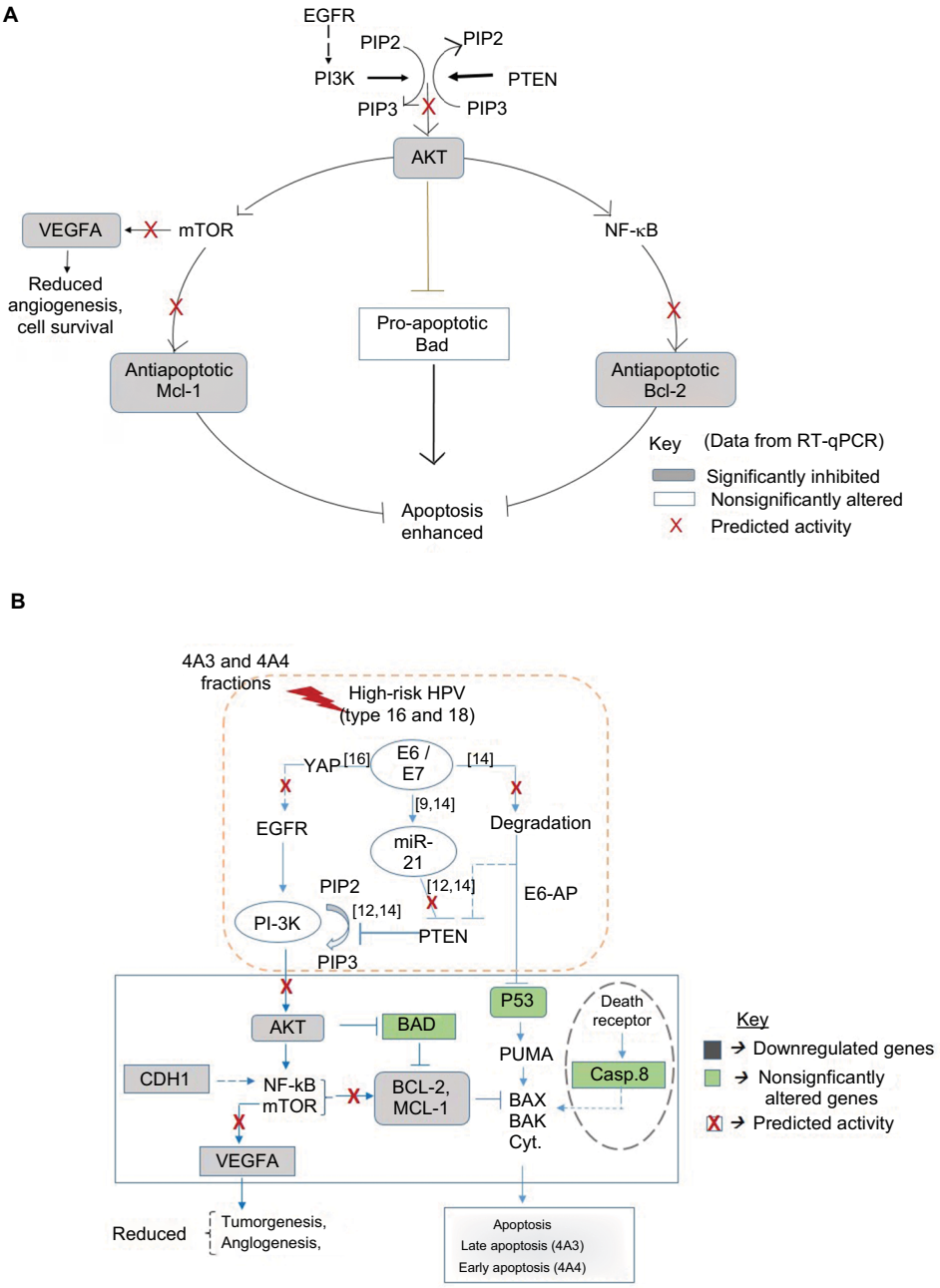

Figure 6 Schematic diagram of molecular network and proposed mechanism of activity.

Notes: (**A**) The predicted mechanism for the reversal of cell survival, angiogenesis, and inhibition of apoptosis. (**B**) Proposed molecular network of interaction as response to treatment. Data supported the activity of 4A3- and 4A4-induced apoptosis, resulting from the inhibition of AKT and antiapoptotic proteins (Mcl-1 and Bcl-2) as well as the VEGFA known for angiogenesis. This implies a possible role by PTEN tumor suppressor against PI3K-AKT pathway. In cervical cancer, PTEN is negatively regulated by miR-21 the expression of which is dependent on HPV E6 oncoprotein for the activation of cell survival, tumorigenesis, angiogenesis, and diminished apoptosis. The data in green and gray shadings indicate the level of expression of genes due to treatment. Data determined by RT-qPCR.

Abbreviations: HPV, human papillomavirus; PI-3K, phosphatidylinositol-3-OH kinase; PTEN, phosphatase and tensin homolog; RT-qPCR, reverse transcriptase quantitative PCR.

Disclosure

The authors report no conflicts of interest in this work.

References

1. Burz C, Berindan-Neagoe I, Balacescu O, Irimie A. Apoptosis in cancer: key molecular signaling pathways and therapy targets. *Acta Oncol*. 2009;48(6):811–821.
2. Irimie AI, Braicu C, Zanoaga O, et al. Epigallocatechin-3-gallate suppresses cell proliferation and promotes apoptosis and autophagy in oral cancer SSC-4 cells. *Onco Targets Ther*. 2015;8:461–470.
3. Berindan-Neagoe I, Braicu C, Tudoran O, Balacescu O, Irimie A. Early apoptosis signals induced by a low dose of epigallocatechin 3-gallate interfere with apoptotic and cell death pathways. *J Nanosci Nanotechnol*. 2012;12(3):2113–2119.
4. Saraste A, Pulkki K. Morphologic and biochemical hallmarks of apoptosis. *Cardiovasc Res*. 2000;45(3):528–537.

5. Lomonosova E, Chinnadurai G. BH3-only proteins in apoptosis and beyond: an overview. *Oncogene*. 2008;27(Suppl 1):S2–S19.
6. Garenne D, Renault TT, Manon S. Bax mitochondrial relocation is linked to its phosphorylation and its interaction with Bcl-xL. *Microb Cell*. 2016;3(12):597–605.
7. Simonyan L, Renault TT, Novais MJ, et al. Regulation of Bax/mitochondria interaction by AKT. *FEBS Lett*. 2016;590(1):13–21.
8. Marte BM, Downward J. PKB/Akt: connecting phosphoinositide 3-kinase to cell survival and beyond. *Trends Biochem Sci*. 1997;22(9):355–358.
9. Kennedy SG, Kandel ES, Cross TK, Hay N. Akt/Protein kinase B inhibits cell death by preventing the release of cytochrome c from mitochondria. *Mol Cell Biol*. 1999;19(8):5800–5810.
10. Bumrungthai S, Ekalaksananan T, Evans MF, et al. Up-Regulation of miR-21 Is Associated with Cervicitis and Human Papillomavirus Infection in Cervical Tissues. *PLoS One*. 2015;10(5):e0127109.
11. Hwang JH, Voortman J, Giovannetti E, et al. Identification of microRNA-21 as a biomarker for chemoresistance and clinical outcome following adjuvant therapy in resectable pancreatic cancer. *PLoS One*. 2010;5(5):e10630.
12. Yao Q, Xu H, Zhang QQ, Zhou H, Qu LH. MicroRNA-21 promotes cell proliferation and down-regulates the expression of programmed cell death 4 (PDCD4) in HeLa cervical carcinoma cells. *Biochem Biophys Res Commun*. 2009;388(3):539–542.
13. Rao Q, Shen Q, Zhou H, Peng Y, Li J, Lin Z. Aberrant microRNA expression in human cervical carcinomas. *Med Oncol*. 2012;29(2):1242–1248.
14. Zheng ZM, Wang X. Regulation of cellular miRNA expression by human papillomaviruses. *Biochim Biophys Acta*. 2011;1809(11–12):668–677.
15. Zaman M, Chauhan N, Yallapu M. Curcumin Nanoformulation for Cervical Cancer Treatment. Sci Rep. 2016;6:20051.
16. Reis PP, Tomenson M, Cervigne NK, et al. Programmed cell death 4 loss increases tumor cell invasion and is regulated by miR-21 in oral squamous cell carcinoma. *Mol Cancer*. 2010;9:238.
17. He C, Mao D, Hua G, et al. The Hippo/YAP pathway interacts with EGFR signaling and HPV oncoproteins to regulate cervical cancer progression. *EMBO Mol Med*. 2015;7(11):1426–1449.
18. Obasi TC, Moldovan R, Toiu A, et al. Molecular-trapping in Emulsion's Monolayer: A New Strategy for Production and Purification of Bioactive Saponins. *Sci Rep*. 2017;7(1):14511.
19. Ekor M. The growing use of herbal medicines: issues relating to adverse reactions and challenges in monitoring safety. *Front Pharmacol*. 2013;4:177.
20. Milrot E, Jackman A, Kniazhanski T, Gonen P, Flescher E, Sherman L. Methyl jasmonate reduces the survival of cervical cancer cells and down-regulates HPV E6 and E7, and survivin. *Cancer Lett*. 2012;319(1):31–38.
21. Xiao JX, Huang GQ, Zhang SH. Soyasaponins inhibit the proliferation of Hela cells by inducing apoptosis. *Exp Toxicol Pathol*. 2007;59(1):35–42.
22. Oh PS, Lim KT. HeLa cells treated with phytoglycoprotein (150 kDa) were killed by activation of caspase 3 via inhibitory activities of NF-kappaB and AP-1. *J Biomed Sci*. 2007;14(2):223–232.
23. Braicu C, Pileczki V, Pop L, et al. Dual targeted therapy with p53 siRNA and Epigallocatechingallate in a triple negative breast cancer cell model. *PLoS One*. 2015;10(4):e0120936.
24. Berindan-Neagoe I, Braicu C, Irimie A. Combining the chemotherapeutic effects of epigallocatechin 3-gallate with siRNA-mediated p53 knock-down results in synergic pro-apoptotic effects. *Int J Nanomedicine*. 2012;7:6035–6047.
25. Podolak I, Galanty A, Sobolewska D. Saponins as cytotoxic agents: a review. *Phytochem Rev*. 2010;9(3):425–474.
26. Cao S, Norris A, Miller JS, et al. Cytotoxic triterpenoid saponins of Albizia gummifera from the Madagascar rain forest. *J Nat Prod*. 2007;70(3):361–366.
27. Haddad M, Laurens V, Lacaille-Dubois MA. Induction of apoptosis in a leukemia cell line by triterpene saponins from Albizia adianthifolia. *Bioorg Med Chem*. 2004;12(17):4725–4734.
28. Mitaine-Offer AC, Pénez N, Miyamoto T, et al. Acylated triterpene saponins from the roots of Securidaca longepedunculata. *Phytochemistry*. 2010;71(1):90–94.
29. Lenz W. Investigation of the root cortex of Securidaca Longepedunculata. *Arb Pharm Inst Univ Berlin*. 1913;10:177.
30. Johnson CT. Taxonomy of the African species of Securidaca (Polygalaceae). *South African Journal of Botany*. 1987;53(1):5–11.
31. Mongalo NI, Mcgaw LJ, Finnie JF, Staden JV, van SJ, Fresen S longipedunculata. Securidaca longipedunculata Fresen (Polygalaceae): a review of its ethnomedicinal uses, phytochemistry, pharmacological properties and toxicology. *J Ethnopharmacol*. 2015;165:215–226.
32. Wee S, Wiederschain D, Maira SM, et al. PTEN-deficient cancers depend on PIK3CB. *Proc Natl Acad Sci U S A*. 2008;105(35):13057–13062.
33. Gagnon V, Mathieu I, Sexton E, Leblanc K, Asselin E. AKT involvement in cisplatin chemoresistance of human uterine cancer cells. *Gynecol Oncol*. 2004;94(3):785–795.
34. Zhang ZC, Tang C, Dong Y, et al. Targeting the long noncoding RNA MALAT1 blocks the pro-angiogenic effects of osteosarcoma and suppresses tumour growth. *Int J Biol Sci*. 2017;13(11):1398–1408.
35. Zhou R, Wei C, Liu J, Luo Y, Tang W. The prognostic value of p53 expression for patients with cervical cancer: a meta analysis. *Eur J Obstet Gynecol Reprod Biol*. 2015;195(Supplement C):210–213.
36. Duerksen-Hughes PJ, Yang J, Ozcan O. p53 induction as a genotoxic test for twenty-five chemicals undergoing in vivo carcinogenicity testing. *Environ Health Perspect*. 1999;107(10):805–812.
37. Zerdoumi Y, Kasper E, Soubigou F, et al. A new genotoxicity assay based on p53 target gene induction. *Mutat Res Genet Toxicol Environ Mutagen*. 2015;789-790(Supplement C):28–35.
38. Jung HS, Rajasekaran N, Ju W, Shin YK. Human Papillomavirus: Current and Future RNAi Therapeutic Strategies for Cervical Cancer. *J Clin Med*. 2015;4(5):1126–1155.
39. Saha B, Adhikary A, Ray P, et al. Restoration of tumor suppressor p53 by differentially regulating pro- and anti-p53 networks in HPV-18-infected cervical cancer cells. *Oncogene*. 2012;31(2):173–186.
40. Fenwick DE, Oakenfull D. Saponin content of soya beans and some commercial soya bean products. *J Sci Food Agric*. 1981;32:273–278.

Supplementary materials

Table S1 Chemical derivatization reaction of 4A3 and 4A4

Serial number	TLC fraction	Chemical derivatization reaction	Color under visible range	Color under UV (365 nm)
i	4A3	10% ethanolic H_2SO_4; heat at 105°C (6 minutes)	Dark green	Brownish
	4A4		Dark green	Yellowish green
ii	4A3	10% ethanolic H_2SO_4; heat at 120°C (15 minutes)	Brownish green	Brownish
	4A4		Dark brown	Brownish
iii	4A3	Antimony III chloride (Carr-Price reaction)	Nil	Pinkish brown
	4A4		Pink/slight purple	Violet
iv	4A3	p-Anisaldehyde–H_2SO_4/heat at 110°C	Brownish	Bluish violet
	4A4		Brownish	Deep bluish violet
v	4A3	Liebermann–Burchard/heat at 110°C (6 minutes)	Slight pink	Pinkish
	4A4		Pinkish	Yellow fluorescent
vi	4A3	Thymol–H_2SO_4 on hydrolyzed substrate; heat at 120°C	Purple	Bluish violet
	4A4		Purple	Bluish violet

Abbreviations: TLC, thin layer chromatography; UV, ultraviolet.

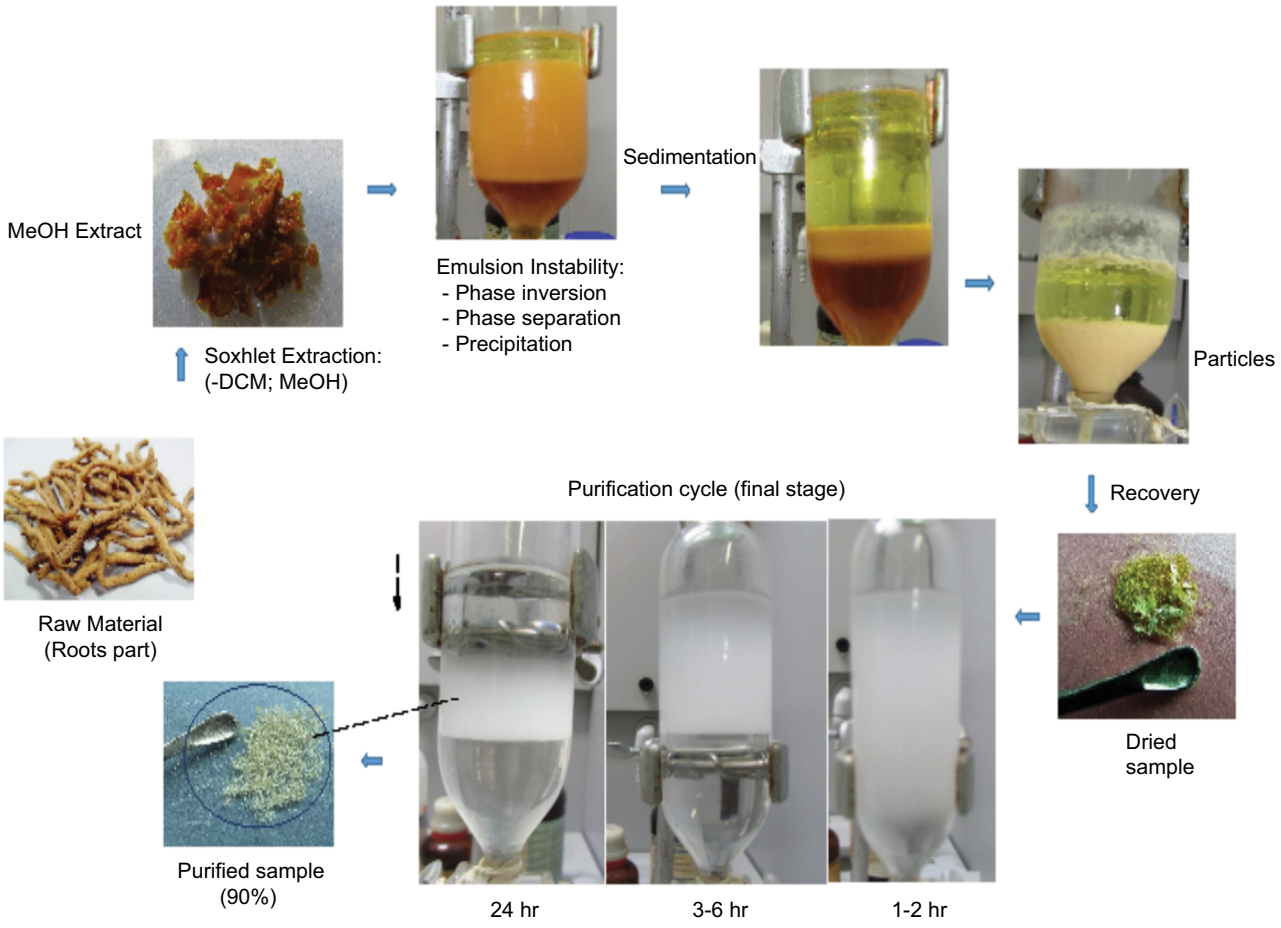

Figure S1 Bioactivity-guided, separation, extraction, and purification by molecular trapping in emulsion's monolayer.
Abbreviation: DCM, dichloromethane.

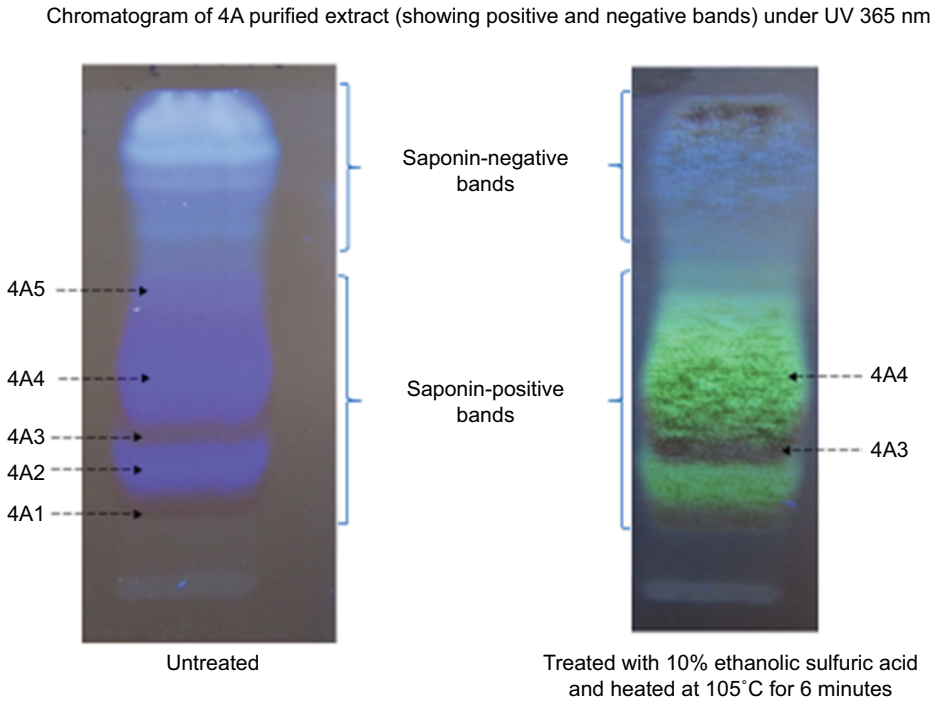

Figure S2 Chromatogram of 4A: separated with RP-C18, F254S in the mobile phase. Methanol:H_2O:formic acid (4:1:0.1). Saponin bands were detected by spraying of 10% ethanolic sulfuric acid plus heat at 105˚C for 6 minutes.
Abbreviation: UV, ultraviolet.

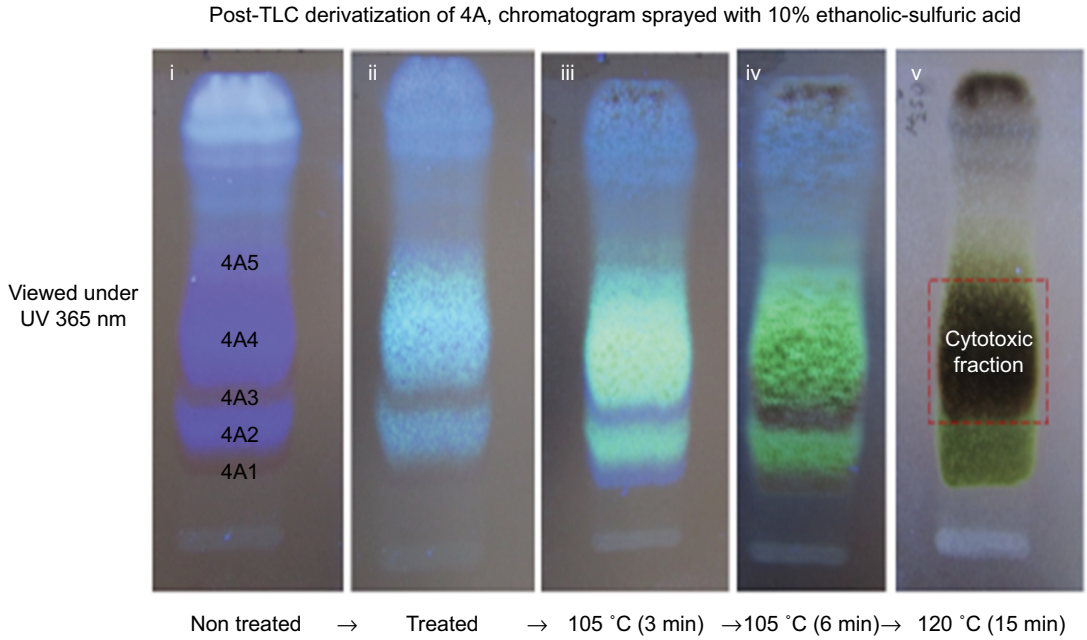

Figure S3 Post-chromatographic derivatization: showing the saponins and the cytotoxic fraction under UV 365 nm. (i) Chromatogram before treatment showing saponins as either blue fluorescent color or transparent colorless band. (ii) After treatment with 10% ethanolic H_2SO_4. (iii) After treatment and heat at 105°C (3 minutes) to detect the colorless saponin bands (4A1 and 4A3) with blue violet color. (iv) Further heating at 105°C which shows greenish yellow fluorescent and dirty green colors for saponin bands (4A2 and 4A4) and (4A1 and 4A3), respectively. (v) The cytotoxic fraction showing dirty green color after heating at 120°C after 10 minutes.
Abbreviations: TLC, thin layer chromatography; UV, ultraviolet.

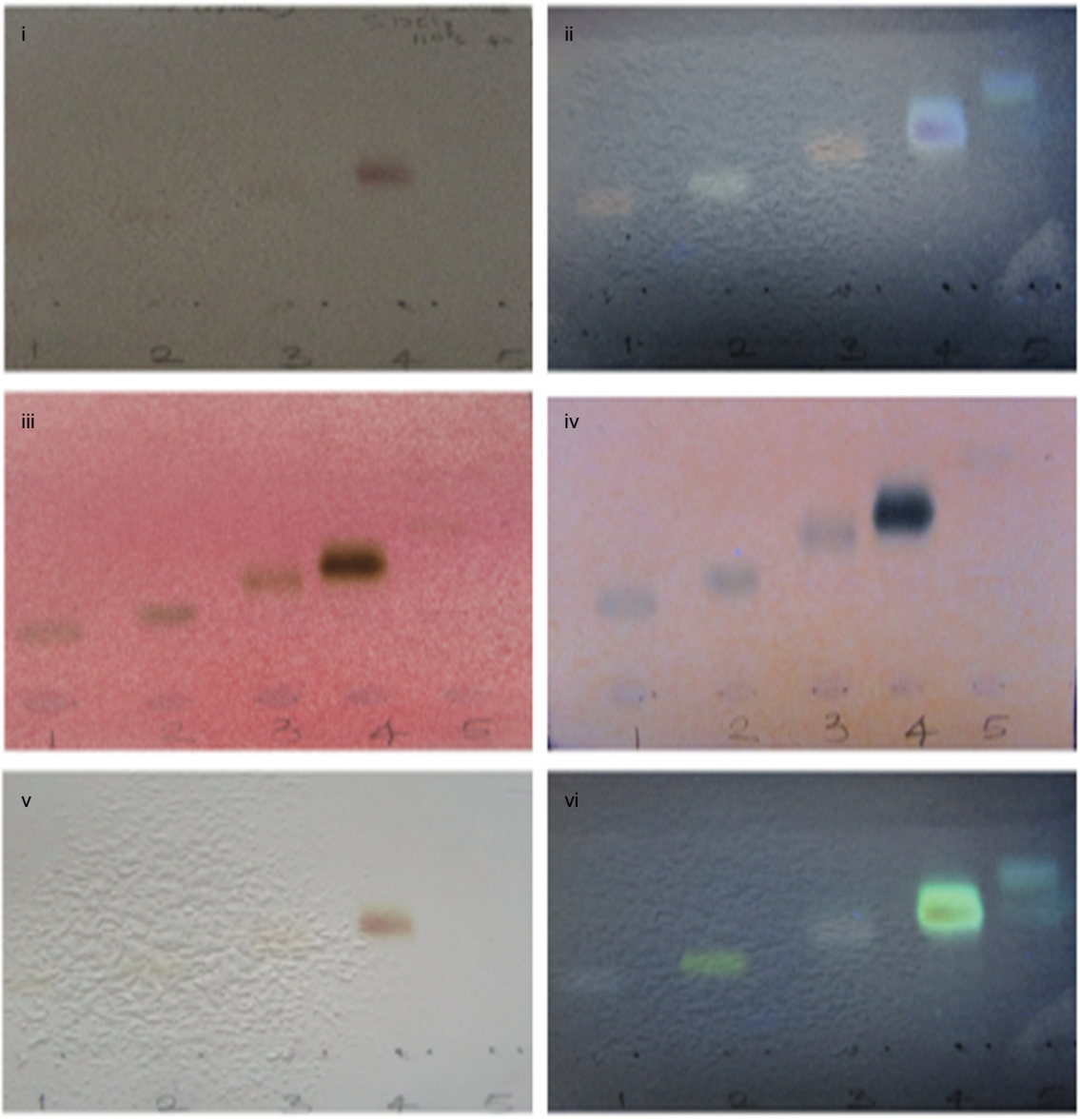

Figure S4 Phytochemical characterization of 4A3 and 4A4. (i, ii) Saponin spots after treating with Carr-Price reagent ($SbCl_3$) at visible and UV 365 nm range, respectively. (iii, iv) Treated with p-anisaldehyde reagent viewed under visible and UV 365 nm, respectively. (v, vi) Treated with Liebermann–Burchard reagent. On heating at 110°C for 6 minutes, Saponin spots were detected. 1, 2, 3, 4, and 5 represent 4A1, 4A2, 4A3, 4A4, and 4A5, respectively.
Abbreviation: UV, ultraviolet.

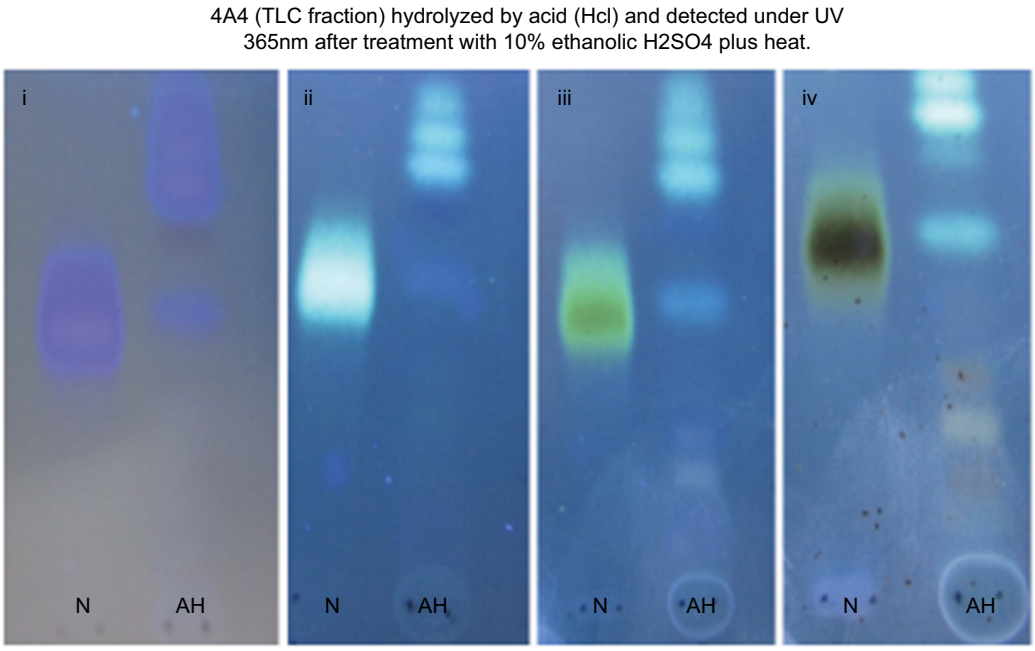

Figure S5 Phytochemical characterization of 4A4. (i) Before treatment. (ii, iii, and iv) Various changes in colors after heating at specific temperatures. The lanes (N) represent non-hydrolyzed 4A4 while AH represents acid-hydrolyzed 4A4 by HCl in reflux system at 70°C for 3 hours.
Notes: (i) Without treatment; (ii) treatment plus heat at 105°C (3 min); (iii) treatment plus heat at 105°C (6 min); (iv) treatment plus heat at 120°C (10–15 min).
Abbreviations: TLC, thin layer chromatography; UV, ultraviolet.